Solid State Communications 253 (2017) 57–62

Contents lists available at ScienceDirect

Solid State Communications

journal homepage: www.elsevier.com/locate/ssc

Communication

The electronic properties, electronic heat capacity and magnetic susceptibility of monolayer boron nitride graphene-like structure in the presence of electron-phonon coupling

Mohsen Yarmohammadi

Young Researchers and Elite Club, Kermanshah Branch, Islamic Azad University, Kermanshah, Iran

ARTICLE INFO

Keywords:
Graphene
Holstein model
Green's function
Density of states
Electronic heat capacity
Magnetic susceptibility

ABSTRACT

In this work, we have studied the influences of electron-phonon (e-ph) coupling and chemical potential on the boron nitride graphene-like sheet. In particular, by starting the Green's function technique and Holstein model, the electronic density of states (DOS), electronic heat capacity (EHC) and magnetic susceptibility (MS) of this system have been investigated in the context of self-consistent second order perturbation theory which has been implemented to find the electronic self-energy. Our findings show that the band gap size decreases (increases) with e-ph coupling (chemical potential) parameters. The Schottky anomaly (crossover) decreases in EHC (MS) as soon as e-ph coupling increases. Also, the corresponding temperature with Schottky anomaly is considerably affected by e-ph coupling.

1. Introduction

Ever since the discovery of a first two-dimensional (2D) material in 2004 [1], graphene, a great interest has appeared in the electronic field because of its unique properties and potential applications [2]. Graphene is a single layer of graphite with two sublattices A and B with the same form, as presented in Fig. 1. In graphene, minimal conductivity in the limit of zero doping (K and K' points, so-called Dirac points) [3] does not input graphene in the technology of electronic devices. Inversion symmetry breaking can create a gap in graphene and integrate graphene into the semiconductor technology [4,5]. On the other hand, Dirac cone structure of graphene generated and opened a door to investigate other 2D materials. Over hundreds of 2D crystals have been found up to now [6–10]. One of the significant compounds in new nanoelectronic devices is the hexagonal boron nitride ($h-BN$) which is an insulating 2D lattice [11]. This compound with a great deal of attention has been applied for a variety of industrial applications such as surface coatings and ceramic composites because of its unique properties including large thermal conductivity, excellent lubricity and chemical inertness [12]. In $h-BN$ structure, boron and nitrogen atoms are bond compartmentally by sp^2 hybridization [13]. This system has a considerable gap of 5.0 eV because of two different boron and nitrogen electronegativities and behaves as a band insulator in the absence of electronic interactions [14,15]. Using *ab-initio* calculations, the electronic transport in BN lattice is investigated which their findings show that the conduction is affected by quantum interference effects for any doping concentration [16].

In 2D electronic materials, electrons interact with bulk and surface phonons [17,18] while in graphene there are 2D in-plane and out-of-plane vibration modes to couple Dirac (spinor) fermions. The stable state of graphene thermodynamically leads to the indeed ripple structures on graphene sheets. The interaction between electrons and optical phonons occurs in two ways. First, the longitudinal optical (LO) and transverse optical (TO) phonons due to the atomic displacement in the plane [19]. Second, out-of-plane vibrations due to the ripple structures which are symmetric with respect to their close atoms. The investigation of optical modes has been done within the Holstein model which are essentially local [20–26]. In graphene and zigzag graphene nanoribbons, e-ph affects DOS measured in scanning tunneling spectroscopy [27,28].

The symmetric property of optical displacements with respect to their close atoms leads to the coupling between electronic density and out-of-plane lattice vibrations [29]. This coupling is an important factor to reduce the electronic mobility and study of electronic properties of gapped graphene-like structures. Considering the coupling of electrons with phonons, study of the charge density wave and superconductivity instabilities is possible [30,31]. Unlike electronic properties, thermal properties in the presence of out-of-plane (Einstein phonons) and e-ph coupling are still not well studied. Due to the specific lattice of this system, the investigation of electronic heat capacity and magnetic susceptibility are notable [33].

The aim of this work is study of the e-ph interaction effects on the

E-mail address: m.yarmohammadi69@gmail.com.

http://dx.doi.org/10.1016/j.ssc.2017.02.003
Received 24 October 2016; Received in revised form 29 December 2016; Accepted 6 February 2017
Available online 07 February 2017

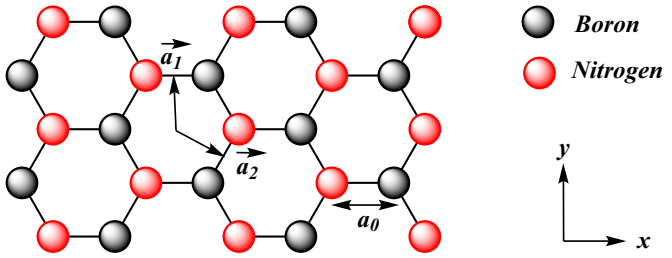

Fig. 1. The boron nitride sheet. The dashed lines illustrate the Bravais lattice unit cell. Each cell includes two atoms labeled by A and B. The primitive vectors are denoted by $\vec{a}_1$ and $\vec{a}_2$, while a_0 denotes inter-atomic distance.

thermodynamic properties of BN graphene-like plane. To treat Einstein phonons, the Boltzman approach is not valid due to their high energies. For this reason, Kubo formula has been applied to find dynamics properties of Dirac fermions [34]. The self-consistent second order perturbation theory is considered to investigate the self-energy of electronic systems. This makes Green's function as a particularly useful tool to describe the effect of e-ph interaction. In this work, DOS, EHC and MS have been studied. The outline of this paper is as follows: In Section 2, we give details about effective Hamiltonian model. In Section 3, we describe the Green's functions and self-consistent perturbation theory. In Section 4, we calculate DOS, temperature dependence of EHC and MS and show the numerical results in Section 5. Finally, our main conclusions are summarized in Section 6.

2. The effective Hamiltonian model

In this section, the electron-lattice coupling with localized Holstein phonons are described as [35]

$$H_0 = (\epsilon_{0A} - \mu)\sum_{i,\sigma} a^\dagger_{i,\sigma}a_{i,\sigma} + (\epsilon_{0B} - \mu)\sum_{i,\sigma} b^\dagger_{i,\sigma}b_{i,\sigma} - t\sum_{i,j,\sigma}(a^\dagger_{i,\sigma}b_{j,\sigma} + h.\,c.\,)$$
$$H_{e-ph} = \omega_0\sum_i c^\dagger_i c_i + g_A\sum_{i,\sigma} a^\dagger_{i,\sigma}a_{i,\sigma}(c^\dagger_i + c_i) + g_B\sum_{i,\sigma} b^\dagger_{i,\sigma}b_{i,\sigma}(c^\dagger_i + c_i) \quad (1)$$

wherein $a_{i,\sigma}(a^\dagger_{i,\sigma})$ annihilates (creates) an electron on the sublattice A with spin σ and $b_{i,\sigma}(b^\dagger_{i,\sigma})$ are for sublattice B. t coefficient in the third term is used to set hopping between nearest neighbor atoms belonging two sublattices A and B and ϵ_{0A}, ϵ_{0B} are the on-site energies of two different sublattice atoms (B and N) and $\epsilon_{0A} - \epsilon_{0B} = 4.5\,eV$ for BN lattice [14,15]. The chemical potential (μ) can be appeared as nonzero in the presence of electron injection by applying the gates which shifts the Fermi energy at Dirac points. ω_0 and g are phonon frequency and e-ph coupling constant, respectively. The out-of-plane optical modes of BN sheet have an energy of $\omega_0 \approx 0.08\,eV$ [33]. In graphene, we have $g_B = g_A$, but because of the inversion symmetry breaking in BN sheet, $g_B = g_A\sqrt{M_A/M_B}$ which $M_{B(A)}$ are the atomic masses. $c_i(c^\dagger_i)$ denotes the annihilation (creation) operator for local phonon modes. In our calculations, we consider units $\hbar = m_e = e = 1$. The primitive unit cell vectors in Fig. 1 are given by

$$\vec{a}_1 = a_0\hat{\mathbf{j}} \quad , \quad \vec{a}_2 = \frac{a_0}{2}(-\hat{\mathbf{j}} + \sqrt{3}\hat{\mathbf{i}}) \quad (2)$$

in which a_0 is inter-atomic distance. Also $\hat{\mathbf{i}}$ and $\hat{\mathbf{j}}$ are unit vectors along the x and y directions, respectively. The Hamiltonian in Eq. (1) can be rewritten after Fourier transformation as

$$H_0(\mathbf{k}) = (\epsilon_{0A} - \mu)\sum_{\mathbf{k},\mathbf{q},\sigma} a^\dagger_{\mathbf{k}+\mathbf{q},\sigma}a_{\mathbf{k},\sigma} + (\epsilon_{0B} - \mu)\sum_{\mathbf{k},\mathbf{q},\sigma} b^\dagger_{\mathbf{k}+\mathbf{q},\sigma}b_{\mathbf{k},\sigma}$$
$$- t\sum_{\mathbf{k},\sigma}(\phi(\mathbf{k})a^\dagger_{\mathbf{k},\sigma}b_{\mathbf{k},\sigma} + h.\,c.\,)H_{e-ph}(\mathbf{k}) = \omega_0\sum_{\mathbf{q}} c^\dagger_{\mathbf{q}}c_{\mathbf{q}}$$
$$+ g_A\sum_{\mathbf{k},\mathbf{q},\sigma} a^\dagger_{\mathbf{k}+\mathbf{q},\sigma}a_{\mathbf{k},\sigma}(c^\dagger_{-\mathbf{q}} + c_{\mathbf{q}}) + g_B\sum_{\mathbf{k},\mathbf{q},\sigma} b^\dagger_{\mathbf{k}+\mathbf{q},\sigma}b_{\mathbf{k},\sigma}(c^\dagger_{-\mathbf{q}} + c_{\mathbf{q}}) \quad (3)$$

where $\phi(\mathbf{k}) = 1 + 2\cos(k_x/2)e^{-ik_y\sqrt{3}/2}$ with momentums $\mathbf{k}$, $\mathbf{q}$ belonging to the first Brillouin zone (FBZ) of honeycomb lattice. The nearest neighbor approximation gives us the following matrix form as

$$H_0(\mathbf{k}) = \begin{pmatrix} \Delta - \mu & t\phi(\mathbf{k}) \\ t\phi^*(\mathbf{k}) & -\Delta - \mu \end{pmatrix} \quad (4)$$

with $\Delta = (\epsilon_{0A} - \epsilon_{0B})/2$. Eigenvalues of the above Hamiltonian can be derived as

$$E_\pm(\mathbf{k}) = \pm\sqrt{(\mu^2 - \Delta^2) + t^2\phi(\mathbf{k})\phi^*(\mathbf{k})} \quad (5)$$

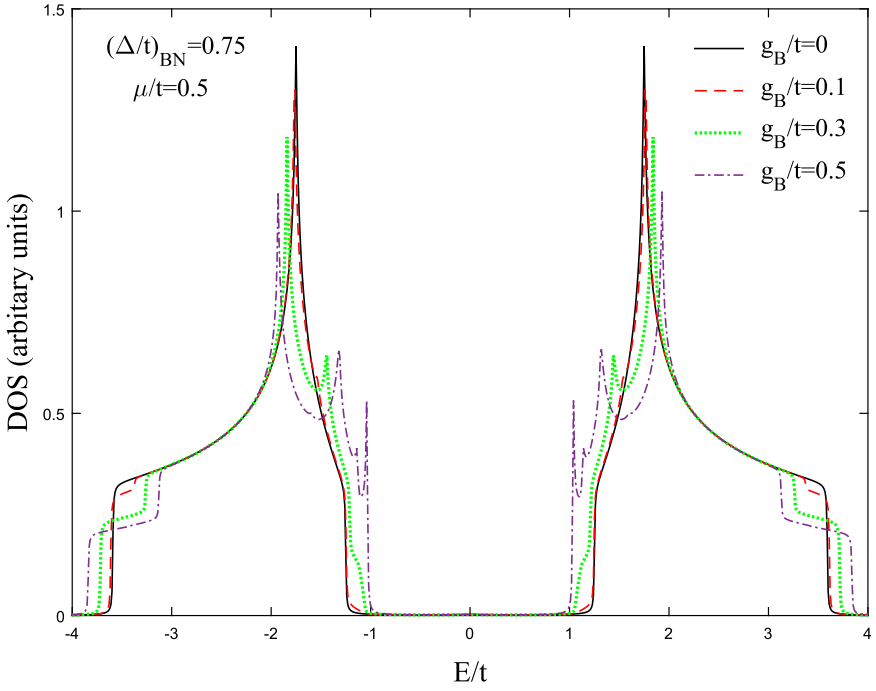

Fig. 2. The total density of states of BN sheet for various e-ph interaction strengths, g_B/t, at $\Delta/t = 0.75$ and $\mu/t = 0.5$.

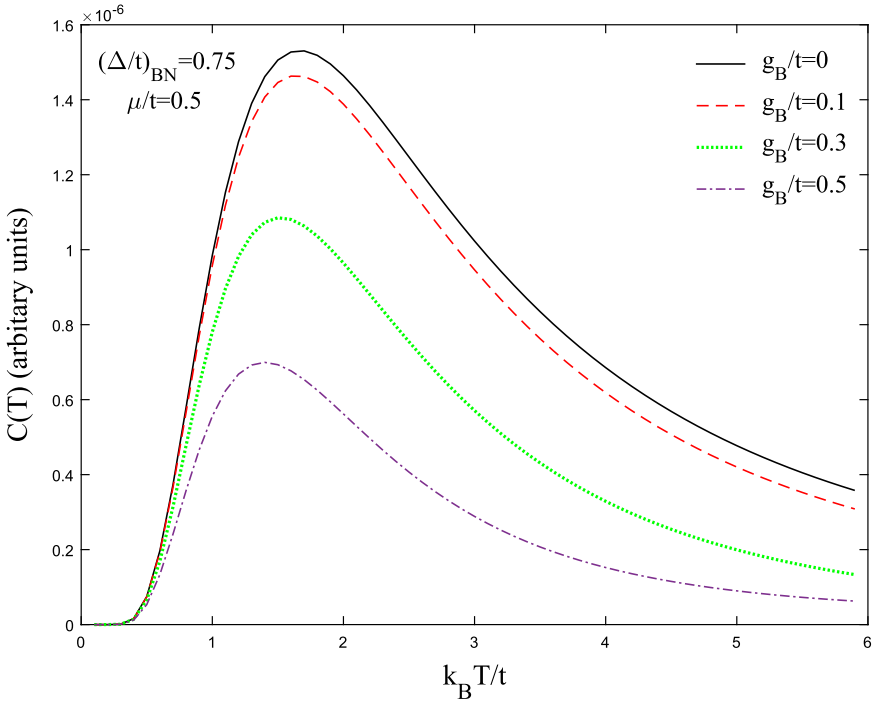

Fig. 3. Temperature dependence of electronic heat capacity of BN sheet for various e-ph interaction strengths, g_B/t, at $\Delta/t = 0.75$ and $\mu/t = 0.5$.

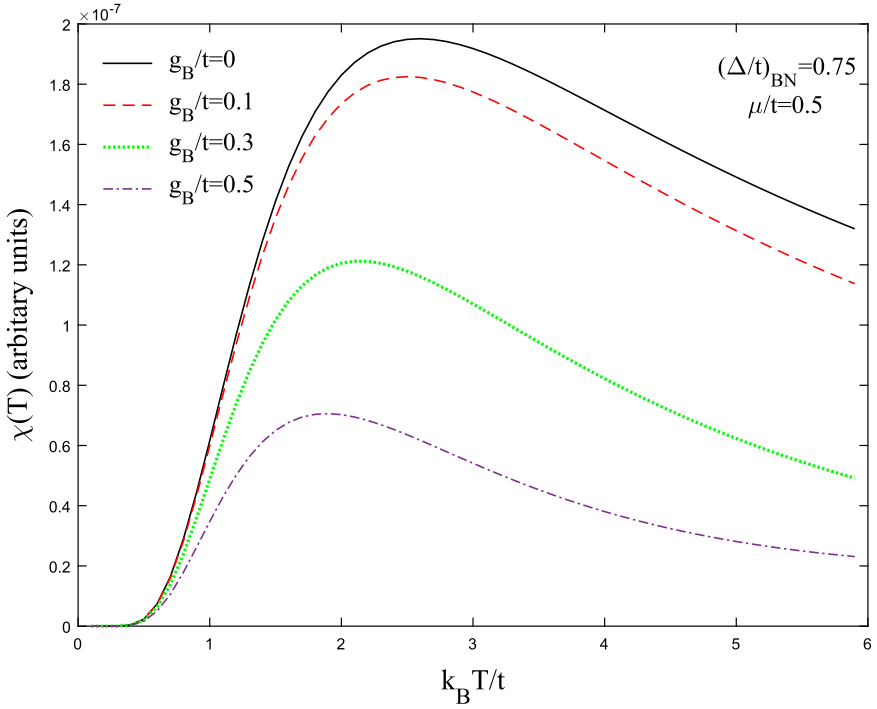

Fig. 4. Temperature dependence of magnetic susceptibility of BN sheet for various e-ph interaction strengths, g_B/t, at $\Delta/t = 0.75$ and $\mu/t = 0.5$.

To derive the Green's function elements, we used the Matsubara formalism [34] and also their Fourier transformation as

$$G_{\alpha\beta'}(\mathbf{k}, \tau') = -\langle T_{\tau'} c_{k,\alpha}(\tau') c^{\dagger}_{k,\beta'}(0)\rangle \; G_{\alpha\beta'}(\mathbf{k}, i\omega_n) = \int_0^{\beta} e^{i\omega_n \tau'} G_{\alpha\beta'}(\mathbf{k}, \tau') d\tau' \tag{6}$$

where β is the inverse of temperature. $c = a(b)$ and α, β' refer to each sublattice atoms A and B. Also τ' is the imaginary time and $\omega_n = (2n + 1)\pi/\beta$ is the Fermionic Matsubara's frequency [34]. The Fourier transformation of unperturbed Green's function matrix of system ($\mathbf{G}_0$) can be defined by [34,36].

$$\mathbf{G}_0(\mathbf{k}, i\omega_n) = \frac{1}{i\omega_n \hat{\mathbf{I}} - H_0(\mathbf{k})} \tag{7}$$

By substituting Eq. (4) into Eq. (7), the Green's function matrix of this system can be found.

3. Green's functions and self-consistent perturbation theory

Green's functions of Dirac fermions in the presence of e-ph coupling are needed to find self-energy diagram. Migdal theorem is used to consider the lowest order perturbation because of the lowest

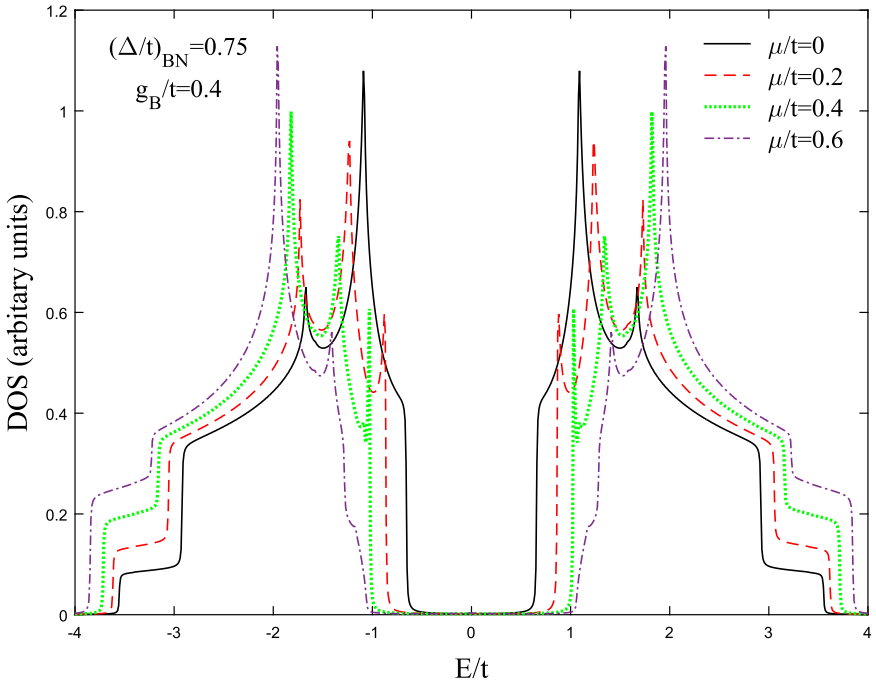

Fig. 5. The total density of states of BN sheet for different values of chemical potentials due to the applied gates at $\Delta/t = 0.75$ and $g_B/t = 0.4$.

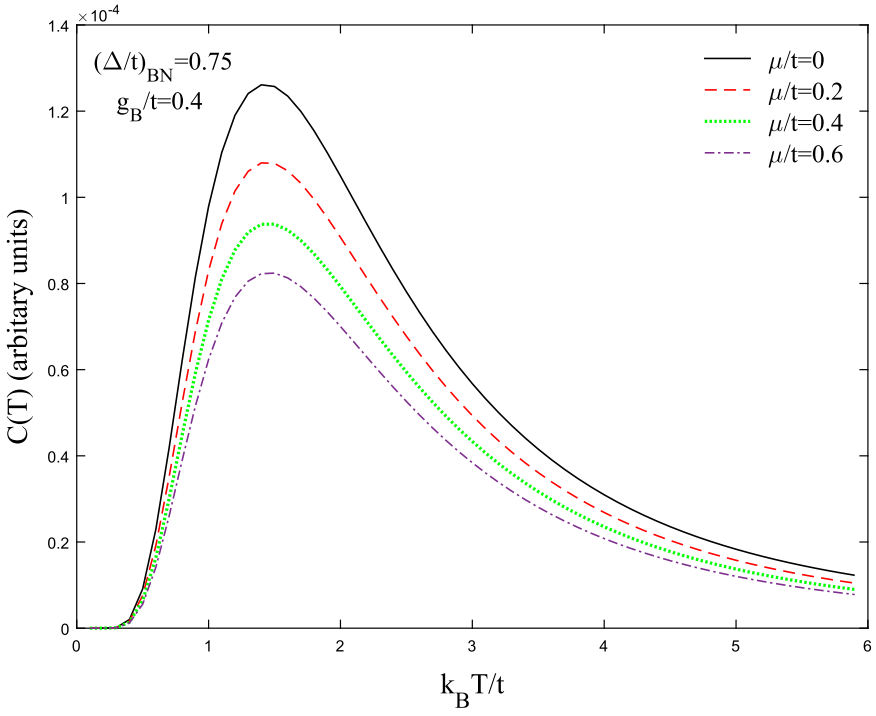

Fig. 6. Temperature behavior of electronic specific heat of BN sheet for different values of chemical potentials due to the applied gates at $\Delta/t = 0.75$ and $g_B/t = 0.4$.

phonon energy scale in comparison with electronic energy scale [37]. Furthermore, we know that the polarization of electron-hole pair can be created by e-ph vertex correction. This theorem let us to neglect it. Unperturbed phononic Green's function is given by

$$D^{(0)}(\mathbf{p}, ip_m) = \frac{2\omega_0}{(ip_m)^2 - \omega_0^2} \tag{8}$$

Also, matrix elements of self-energy, $\sum_{\gamma\gamma}(\mathbf{k}, i\omega_n)$, at second order perturbation theory are given by means of the Feynman rule [34]

$$\Sigma_{\gamma\gamma}(\mathbf{k}, i\omega_n) = -\frac{1}{\beta}\sum_{p,m} g_\gamma^2 D^{(0)}(\mathbf{p}, ip_m) G_{\gamma\gamma}(\mathbf{k}-\mathbf{p}, i\omega_n - ip_m) \tag{9}$$

Interacting Green's function is related to the spectral function based on the Lehman representation [34] as

$$G_{\gamma\eta}(\mathbf{k}, i\omega_n) = \int_{-\infty}^{+\infty} \frac{d\omega}{2\pi} \frac{\mathcal{A}_{\gamma\eta}(\mathbf{k}, \omega)}{i\omega_n - \omega} \mathcal{A}_{\gamma\eta}(\mathbf{k}, \omega) = -2\Im G_{\gamma\eta}(\mathbf{k}, i\omega_n \longrightarrow E + i0^+) \tag{10}$$

where $\mathcal{A}(\mathbf{k}, \omega)$ is the electronic spectral function matrix. By substituting Eq. (10) into Eq. (9) and applying Matsubara's frequency summa-

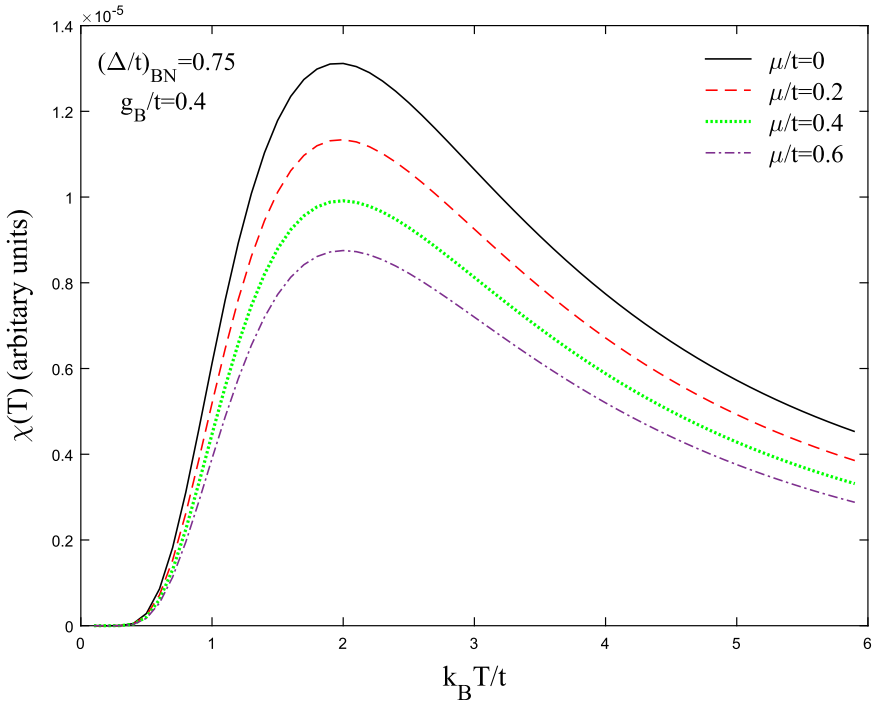

Fig. 7. Temperature behavior of magnetic susceptibility of BN sheet for different values of chemical potentials due to the applied gates at $\Delta/t = 0.75$ and $g_B/t = 0.4$.

tion rule, self-energy matrix element can be given by

$$\Sigma_{\gamma\gamma}(\mathbf{k}, i\omega_n) = \frac{1}{2N}\sum_{p,\alpha} g_\alpha^2 \int_{-\infty}^{+\infty} \frac{dE}{2\pi}\left(\frac{n_B(\omega_0) + n_F(E)}{i\omega_n - E + \omega_0} + \frac{n_B(\omega_0) + 1 - n_F(E)}{i\omega_n - E - \omega_0}\right) \mathcal{A}_{\gamma\gamma}(\mathbf{k} - \mathbf{p}, E) \tag{11}$$

where $n_F(E) = 1/(e^{\beta E} + 1)$ and $n_B(\omega_0) = 1/(e^{\beta\omega_0} - 1)$ are Fermi-Dirac and Bose-Einstein distribution functions, respectively. Summation in Eq. (11) is also performed over $\mathbf{k}$ points belonging to the FBZ. Finally, the perturbed Green's function in the Matsubara's notation is given by [34]

$$G'(\mathbf{k}, i\omega_n) = G(\mathbf{k}, i\omega_n) + G(\mathbf{k}, i\omega_n)\Sigma(\mathbf{k}, i\omega_n)G'(\mathbf{k}, i\omega_n) \tag{12}$$

4. Electronic density of states, electronic heat capacity and magnetic susceptibility

The DOS can be derived by tracing over the imaginary part of Green's functions, $D(E) = -\Im TrG(E)/\pi$ [38,39]. By engaging Eqs. (4) and (7) and setting $i\omega_n \to E + i0^+$ as a numerical calculation in which 0^+ is a very small real number, total DOS is given by

$$D(E) = -\frac{1}{2\pi N_c}\sum_{\zeta,\mathbf{k}} \Im G'_{\zeta\zeta}(\mathbf{k}, E + i0^+) \tag{13}$$

where ζ describe a sub-site and N_c is the number of atoms per unit cell. The EHC could be introduced by following expression [34]

$$C(T) = \int_{-\infty}^{+\infty} dE E D(E)\partial_T f(E) \tag{14}$$

in which $D(E)$ displays the DOS of Bloch electrons calculated by Eq. (13). Calling Eqs. (13) and (14), EHC would be obtained by

$$C(T) = -\frac{1}{2\pi N_c T^2}\sum_{\zeta,\mathbf{k}} \Im \int_{-\infty}^{+\infty} dE \frac{E^2 e^{(E-\mu)/k_BT}}{(e^{(E-\mu)/k_BT} + 1)^2} G'_{\zeta\zeta}(\mathbf{k}, E + i0^+) \tag{15}$$

For a monolayer BN sheet, the MS which is response of the system to the applied external magnetic field can be calculated as [35]

$$\chi(T) = -\int_{-\infty}^{+\infty} dE D(E)\partial_E n_F(E) \tag{16}$$

Using Eqs. (13) and (16), the MS would be introduced

$$\chi(T) = -\frac{1}{2\pi NT}\sum_{\mathbf{k},\zeta} \Im \int_{-\infty}^{+\infty} dE \frac{e^{(E-\mu)/T}}{(e^{(E-\mu)/T} + 1)^2} G'_{\zeta\zeta}(\mathbf{k}, E) \tag{17}$$

The study of $\chi(T)$ and $C(T)$ behaviors of this lattice in the presence of e-ph interaction is the main aim of this work. In the next section, the results are presented.

5. Numerical results

Density of states for BN sheet versus energy for various e-ph couplings at $k_BT/t = 0.01$ has been plotted in Fig. 2. The presence of e-ph coupling acts as a perturbation in the system and we expect to see some changes in DOS due to the perturbed quantum states. At first view, one can see that the band gap is decreasing with e-ph coupling. In fact, the energy gap is corresponding to the vanished quasiparticle weight of electronic excitation spectrum which is observed in the range $-1.2 < E/t < 1.2$. Van-Hove singularities are the result of degenerated quantum states. According to this figure, the spectrum is smeared starting from the Van-Hove singularities at $|E| = 1.75t$, and the smeared area expands around their vicinal regions when g/t is increased. Also, DOS is symmetric in terms of energy, i.e., $D(E) = D(-E)$ at finite nonzero value for gap and chemical potential in each of positive or negative energy regions. On the other hand, we know that the total number of available states corresponds to the area under the curve of DOS which is proportional to the electronic density of system. Therefore, in spite of relative changes in DOS, the area under the curves remains constant.

Figs. 3 and 4 illustrate a soft peak in the EHC (known as Schottky anomaly) and magnetic susceptibility of the system. More importantly, in the presence of e-ph coupling the position of this anomaly moves towards the lower temperatures because of the decreased band gap size in DOS and its height shifts down when e-ph coupling is increased. These behaviors are in agreement with the theory of EHC. It is well-known that the EHC of semiconductors at low temperatures can be written as $C(T) \propto e^{-\Delta/T}$ [40,41]. According to this formula, $C(T)$

increases at low temperature region with Δ, as shown in Fig. 3. On the other hand, it decreases at high temperature region. In this region, by increasing the temperature less value of energy is needed to conductance rather than low temperature region. Fig. 4 shows that there is a crossover which parts the temperature dependence of susceptibility of system into two temperature regions. Before (after) the crossover, the susceptibility increases (decreases) with temperature. This crossover is due to the Van-Hove singularities in DOS where one can see it can be analyzed with the mathematically relation between $\chi(T)$ and $D(E)$ in (17). Before the crossover, the magnetic ordering reduces due to quantum fluctuations with temperature. After the crossover, thermal fluctuations are dominant and more important than quantum fluctuations which lead to the reduction of susceptibility at high temperatures.

In Figs. 5, 6 and 7, the electronic properties of undoped and doped BN sheet in presence of the e-ph coupling have been compared. Fig. 5 shows that the band gap of system increases with chemical potential which is reasonable due to the increasing of quantum states after turning on the gates and also increasing of the scattering rate. Figs. 6 and 7 have the same behaviors with temperature based on the mentioned reasons and equations for EHC and MS. In these figures, EHC and MS of the system decrease when the gates are applied to induce chemical potential. $C(T)$ and $\chi(T)$ are decreased because of the increase of scattering effects. In fact, there is a slightly shift in their peaks, but because of the considered strong e-ph coupling, $g/t = 0.4$, this shift is very small in plots and seems that there is not any shifting in the place of crossover.

6. Conclusions

To sum up, Green's function approach has been used to study the full band electronic structure and thermodynamic properties of BN lattice in the presence of Einstein phonons and electron-phonon coupling. The effect of electron-phonon coupling and chemical potential on temperature dependence of electronic heat capacity and magnetic susceptibility are studied. It is concluded that the band gap of system decreases with electron-phonon interaction and increases with chemical potential due to the change of quantum quasistates. For all of temperature regions, the electron-phonon causes the enhancement of Schottky anomaly in electronic heat capacity and crossover of curves in magnetic susceptibility which appear at low temperatures. The crossover decreases with chemical potential without any shifting.

References

[1] K.S. Novoselov, A.K. Geim, S.V. Morozov, D. Jiang, Y. Zhang, S.V. Dubons, I.V. Grigorieva, A.A. Firsov, Science 306 (2004) 666.
[2] A.K. Geim, K.S. Novoselov, Nat. Mater. 6 (2007) 183.
[3] G.W. Semenoff, Phys. Rev. Lett. 53 (1984) 2449.
[4] Y. Lin, K.A. Jenkins, A. Valdes-Garcia, J.P. Small, D.B. Farmer, P. Avouris, Nano Lett. 9 (2009) 422.
[5] J. Kedzierski, P. Hsu, P. Healey, P.W. Wyatt, C.L. Keast, M. Sprinkle, C. Berger, W.A. de Heer, IEEE Trans, Electron Devices 55 (2008) 2078.
[6] S.Z. Butler, S.M. Hollen, L.Y. Cao, et al., ACS Nano 7 (2013) 2898.
[7] M.S. Xu, T. Liang, M.M. Shi, et al., Chem. Rev. 113 (2013) 3766.
[8] S. Cahangirov, M. Topsakal, E. Akturk, et al., Phys. Rev. Lett. 102 (2009) 236804.
[9] D. Malko, C. Neiss, F. Vines, et al., Phys. Rev. Lett. 108 (2012) 086804.
[10] H.Q. Huang, W.H. Duan, Z.R. Liu, New. J. Phys. 15 (2013) 023004.
[11] Q.H. Wang, K. Kalantar-Zadeh, A. Kis, J.N. Coleman, M.S. Strano, Nat. Nanotechnol. 7 (2012) 699.
[12] J. Eichler, C. Lesniak, J. Eur. Ceram. Soc. 28 (2008) 1105.
[13] N. Alem, et al., Phys. Rev. B 80 (2009) 155425.
[14] T.K. Pauli, P. Bhattacharya, D.N. Bose, Appl. Phys. Lett. 56 (1990) 2648.
[15] C.H. Jin, F. Lin, K. Suenaga, S. Iijima, Phys. Rev. Lett. 102 (2009) 195505.
[16] A. Lherbier, X. Blase, Y. Niquet, F. Triozon, S. Roche, Phys. Rev. Lett. 101 (2008) 036808.
[17] W. Xiaoguang, F.M. Peeters, J.T. Devreese, Phys. Rev. B 31 (1985) 3420; S. Das Sarma, B.A. Mason, Ann. Phys. 163 (1985) 78.
[18] A.K. Sood, J. Menendez, M. Cardona, K. Ploog, Phys. Rev. Lett. 54 (1985) 2111; C. TralleroGiner, F. Garca-Moliner, V.R. Velasco, M. Cardona, Phys. Rev. B 45 (1992) 11944; A.J. Shields, M. Cardona, K. Eberl, Phys. Rev. Lett. 72 (1994) 412.
[19] W.P. Su, J.R. Schrieffer, A.J. Heeger, Phys. Rev. Lett. 42 (1979) 1698.
[20] G.L. Goodvin, M. Berciu, G.A. Sawatzky, Phys. Rev. B 74 (2006) 245104.
[21] T. Holstein, Ann. Phys. 8 (1959) 325.
[22] T. Holstein, Ann. Phys. 8 (1959) 343.
[23] S. Piscanec, et al., Phys. Rev. Lett. 93 (2004) 185503.
[24] S. Piscanec, et al., Phys. Rev. B 75 (2007) 035427.
[25] S. Pisana, et al., Nat. Mater. 6 (2007) 198.
[26] Kh. Jahanbani, R. Asgari, Eur. Phys. J. B 73 (2010) 247.
[27] G. Li, A. Luican, E.Y. Andrei, Phys. Rev. Lett. 102 (2009) 176804.
[28] K. Sasaki, K. Sato, J. Jiang, R. Saito, S. Onari, Y. Tanaka, Phys. Rev. B 75 (2007) 235430.
[29] W.P. Su, J.R. Schrieffer, A.J. Hoger, Phys. Rev. Lett. 42 (1979) 1698.
[30] D. Sanchez-Portal, E. Artacho, J.M. Soler, A. Rubio, P. Ordejo'n, Phys. Rev. B. 59 (1999) 12678.
[31] M.S. Dreesselhaus, P.C. Eklund, Adv. Phys. 49 (2000) 705.
[33] S. Jung, M. Park, J. Park, T. Jeons, H. Kim, K. Watanabe, T. Tanignchi, D. Ha, Ch. Huang, Y. Kim, Sci. Rep. 5 (2015) 16642.
[34] G.D. Mahan, Many Particle Physics, Plenum Press, New York, 1993.
[35] W. Nolthing, A. Ramakanth, Quantum Theory of Magnetism, Springer, New York, 2009.
[36] M. Yarmohammadi, Solid State Commun. 234 (2016) 14.
[37] A.B. Migdal, I. Zhurnal Eksperimentalnoi, Teor. Fiz. 34 (1958) 1438.
[38] G. Grosso, G.P. Parravicini, Solid State Physics, 2nd edn., Academic Press, New York, 2014.
[39] M. Yarmohammadi, J. Magn. Magn. Mater. 417 (2016) 208.
[40] C. Kittle, Introduction to Solid State Physics, eighth ed. Wiley, New York, 2004.
[41] R.K. Pathria, Statistical Mechanics, Oxford Press, London, 1997.